POWER DIVIDERS

POWER DIVISION

POWER SPLITTERS

TEE JUNCTION

Electric circuits, systems, and devices frequently require channeling portions of energy to different locations within a particular physical system. This requirement generally occurs in most electrical systems operating from very low (dc) to very high (optical) frequencies. Indeed, the typical potential divider used in bias supplies represents such an application at low frequencies, and at optical frequencies the beam splitter is a frequently used device that divides the energy into separate channels. Additionally, the multiplexer represents a power division device based primarily on separation of power into specific frequency bands at ideally comparable powers. The concept of power division finds, perhaps, its broadest application in higher frequency systems and devices where design concepts are typically discussed in terms of power flow and transmission. Efficient power divider design is absolutely essential in the realization of such electronic structures.

In providing power division, a signal having power P_1 is inserted into the input of a circuit as shown in Fig. 1. The outputs are split into P_2 and P_3. The more general case is illustrated in Fig. 2. Here a signal with power P_1, which may cover a band of frequencies $f + \Sigma_i \Delta f_i$ is injected. Output signals are then required over distinct subfrequency bands $f + \Delta f_1 + \Delta f_2$ and so on, at different power levels in each subband.

The following sections cover the design and analysis of such power division devices over bands of frequency ranging from dc to optical. Finally, it should be emphasized that such power dividers can also be used for power combining.

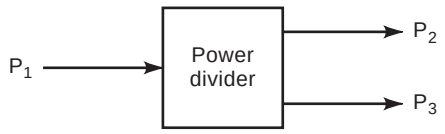

Figure 1. 3-port power divider: Input power $P_1 = P_2 + P_3$ (sum of two output powers).

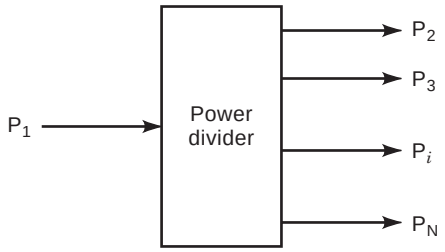

Figure 2. N-port power divider: Input power $P_1 = P_2 + P_3 + \ldots P_N$ (sum of $N - 1$ output powers).

CIRCUIT ELEMENTS UTILIZED IN POWER DIVIDER DESIGN

In order to discuss power divider analysis and design, it is first necessary to describe the types of constituent circuit elements utilized in device realization. Electrical power transmission systems can be very broadly classified according to the frequency of transmission, which ranges from dc (0 Hz) to optical frequencies (terahertz). Some typical elements (1) used for the transmission of electrical power and in the design of dividers are listed in what follows and graphically illustrated in Fig. 3.

Open Two-Wire Transmission Line

This two-wire line is used mainly at lower frequencies ($<$ 500 MHz) over short distances, for example, to connect a television antenna to a receiver. Its main drawback is that it is unshielded and radiates electromagnetic energy.

Coaxial Transmission Line

The major application of coaxial transmission lines is in the cable television industry, connecting the transmitting station to widely distributed subscribers. Because the inner conductor is shielded by the outer common conductor, the electric and magnetic fields are confined to the region between concentric conductors; thus the problem of radiation is avoided. It is used widely as a high-frequency transmission line, for both low-power and high-power operation up to $\sim$ 3 GHz, and for low-power applications in the range from X band (8 GHz to 12 GHz) to Ka band (26 GHz to 40 GHz).

Rectangular and Circular Waveguides

Waveguide transmission lines are also shielded due to their structure, and are more widely used at higher microwave frequencies of above 5 GHz. They can handle higher powers than coaxial lines with lower loss per unit length of the line.

Microstrip Line

The microstrip configuration has become increasingly important in the fabrication of microwave integrated circuits due to the development of low-loss, high-dielectric materials. The microstrip line is an asymmetrical structure consisting of a thin conductor and a ground plane separated by a low-loss dielectric material.

Stripline

Strip transmission lines are used in the design and fabrication of modern radiofrequency (*RF*) and microwave systems. Basically, the energy is transmitted through a low-loss dielectric material.

The stripline configuration consists of a center conducting strip and a pair of ground planes placed symmetrically on either side of the center conductor. The two ground planes are usually shorted together with screws or rivets to prevent any radiation leakage through the sides.

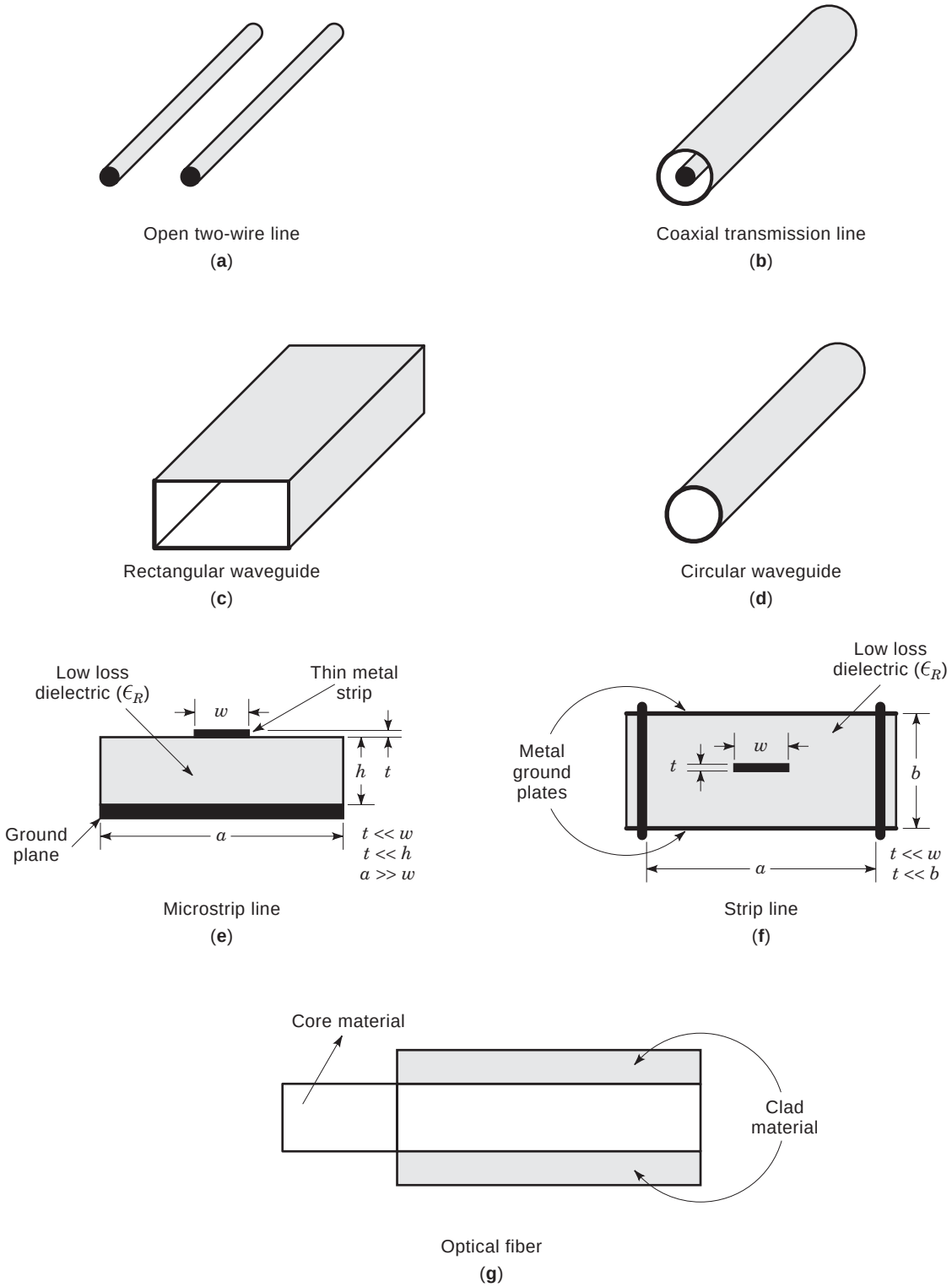

Figure 3. Typical transmission lines. (a) Open two-wire line; (b) Coaxial line; (c) Rectangular waveguide; (d) Circular waveguide; (e) Microstrip line; (f) Stripline; (g) Optical fiber.

Optical Fiber

A fiber-optic transmission line consists of a thin glass fiber for the efficient transmission of light; it is widely used in short links for telephone and computer communication circuits.

POWER DIVIDER CONFIGURATIONS, ANALYSIS AND DESIGN TECHNIQUES

Power dividers and combiners are essentially multiport junctions consisting of one of the different transmissions

line types listed in the previous section. They are utilized in the design of important components, such as filters, antennas, mixers, and duplexers. Power dividers can be broadly classified according to the frequency of the signal transmitted through the network system.

A typical power divider configuration is shown in Fig. 4. To discuss the design of such structures, it is first necessary to describe some of the analysis technique that are essential to the presentation of actual designs.

ANALYSIS TECHNIQUES FOR POWER DIVIDER NETWORKS

The generalized N port network shown in Fig. 4 (2) is driven by a signal generator V_g at port 1, and the other ports terminate in normalized load impedances z_k. The different approaches to input-output analysis of this network are presented in the following discussion.

Impedance/Admittance Matrix Analysis

The N port network can be described electrically in terms of its $N \times N$ impedance matrix as

$$\begin{bmatrix} V_1 \\ V_2 \\ \vdots \\ V_N \end{bmatrix} = \begin{bmatrix} Z_{11} & Z_{12} & Z_{13} & \dots & Z_{1N} \\ Z_{21} & Z_{22} & Z_{23} & \dots & Z_{2N} \\ \vdots & & & & \\ Z_{N1} & Z_{N2} & Z_{N3} & \dots & Z_{NN} \end{bmatrix} \begin{bmatrix} I_1 \\ I_2 \\ \vdots \\ I_N \end{bmatrix} \tag{1}$$

where the individual impedance parameters are defined by terminating the ports in open circuit loads as follows:

$$Z_{jk} = \frac{V_j}{I_k}, I_j = 0, j \neq k \tag{2}$$

and

$$Z_{jj} = \frac{V_j}{I_j}, I_k = 0, j \neq k \tag{3}$$

The corresponding admittance matrix of the N-port can be written as

$$\begin{bmatrix} I_1 \\ I_2 \\ \vdots \\ I_N \end{bmatrix} = \begin{bmatrix} Y_{11} & Y_{12} & Y_{13} & \dots & Y_{1N} \\ Y_{21} & Y_{22} & Y_{23} & \dots & Y_{2N} \\ \vdots & & & & \\ Y_{N1} & Y_{N2} & Y_{N3} & \dots & Y_{NN} \end{bmatrix} \begin{bmatrix} V_1 \\ V_2 \\ \vdots \\ V_N \end{bmatrix} \tag{4}$$

where the individual admittance parameters are defined by terminating the ports in short circuit loads as follows:

$$Y_{jk} = \frac{I_j}{V_k}, V_j = 0, j \neq k \tag{5}$$

and

$$Y_{jj} = \frac{I_j}{V_j}, V_k = 0, j \neq k \tag{6}$$

Scattering Matrix Analysis of N-Port Power Divider Networks

The scattering parameters of a network are also a set of quantities that are frequently used to characterize an electrical network. This analysis approach is particularly convenient for handling the problem of power transfer from a finite impedance generator to a complex load. Another advantage of the latter approach is that every linear, passive, time-invariant network possesses a scattering matrix, whereas some networks possess neither an impedance matrix nor an admittance matrix. The incident and reflected waves at the kth port, as shown in Fig. 4 are denoted by a_k and b_k respectively. Then the scattering matrix of the N-port can be written as

$$\begin{bmatrix} b_1 \\ b_2 \\ \vdots \\ b_N \end{bmatrix} = \begin{bmatrix} S_{11} & S_{12} & S_{13} & \dots & S_{1N} \\ S_{21} & S_{22} & S_{23} & \dots & S_{2N} \\ \vdots & & & & \\ S_{N1} & S_{N2} & S_{N3} & \dots & S_{NN} \end{bmatrix} \begin{bmatrix} a_1 \\ a_2 \\ \vdots \\ a_N \end{bmatrix} \tag{7}$$

where a_k and b_k are defined in terms of port voltages and currents as

$$a_k = \frac{1}{2\sqrt{r_k}}[V_k + z_k I_k]$$

$$b_k = \frac{1}{2\sqrt{r_k}}[V_k + z_k^* I_k]$$

The individual scattering parameters are defined by terminating the ports in matched loads as follows:

$$S_{jk} = \frac{b_j}{a_k}, a_j = 0, j \neq k \tag{8}$$

and

$$S_{jj} = \frac{b_j}{a_j}, a_k = 0, j \neq k \tag{9}$$

POWER DIVIDER DESIGNS

This section discusses the practical realization of power divider circuits that operate in the different frequency ranges encountered in power transmission. Although these devices are based on the same underlying N-port network analysis, their physical structures will be seen to be very diverse depending upon the frequency of transmission.

Direct Current and Low-Frequency Power Dividers (0 MHz to 20 MHz)

This section discusses the design of those power dividers used mostly in the transmission and distribution of electrical power. These low-frequency power dividers are fabricated essentially from lumped circuit elements that operate well at dc and low frequencies of up to $\sim$ 20 MHz.

Resistive Series and Parallel Networks. The simplest N-port power divider type is shown in Fig. 5. It consists of a series connection of an independent voltage source V driv-

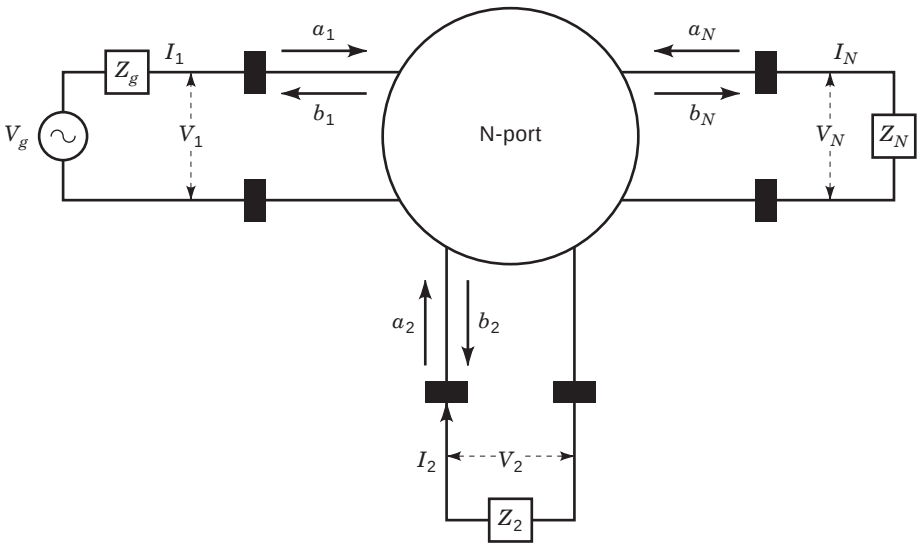

Figure 4. Schematic of N-port power divider: V, I, a, and b represent the voltage, current, incident, and reflected voltage waves, respectively.

ing N resistors $R_1, R_2 \ldots R_N$ and is termed a *voltage divider.* The series current I is given by

$$I = \frac{V}{R}$$

where

$$R = R_1 + R_2 + R_3 + \ldots R_N$$

The instantaneous input power $P = VI$ is divided among the N resistors

$$P = P_1 + P_2 + P_3 \ldots + P_N \tag{10}$$

where the power dissipated by the kth resistor P_k is given by

$$P_k = I^2 R_k \text{ watt} \tag{11}$$

From Eqs. (13) and (11) it follows that the power division ratio can be written as

$$P_1 : P_2 : P_3 : \ldots : P_N = R_1 : R_2 : R_3 \ldots R_N \tag{12}$$

A similar divider, which is shown in Fig. 6, consists of a parallel connection of N resistors driven by an independent current source I. Such a circuit is called a *current divider,* and the shunt voltage across each resistor is given by

$$V = I_k R_k, k = 1, 2, 3 \ldots N$$

where I_k is the current in the kth resistor. The power dissipated in the kth resistor is given by

$$P_k = I_k^2 R_k \tag{13}$$

and substituting $I_k = V/R_k$ into Eq. (17), we obtain the power divider ratios as

$$P_1 : P_2 : P_3 : \ldots : P_N = \frac{1}{R_1} : \frac{1}{R_2} : \frac{1}{R_3} \cdots \frac{1}{R_N} \tag{14}$$

The 3-Port T Junction Power Divider. The 3-port T junction, a fundamental passive component in electrical circuits, can be used either as a power divider or as a power combiner. The T junction and other multiport circuits are effectively analyzed by the power scattering matrix formulation. In this formulation, the T junction shown in Fig. 7, which could represent a two-wire, coaxial, waveguide or microstrip junction, is modeled as a lossless, reciprocal and symmetrical 3-port network. The model can be described in terms of a 3-port scattering matrix as follows (2):

$$[S] = \begin{bmatrix} S_{11} & S_{12} & S_{13} \\ S_{21} & S_{22} & S_{23} \\ S_{31} & S_{32} & S_{33} \end{bmatrix} \tag{15}$$

For the case of a lossless, passive network, the power condition is (20)

$$[S]^T [S]^* = [I] \tag{16}$$

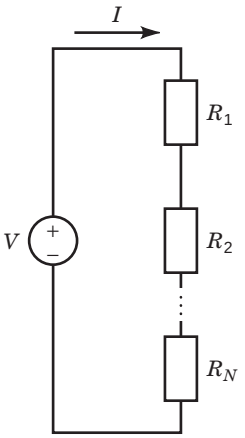

Figure 5. Series voltage divider.

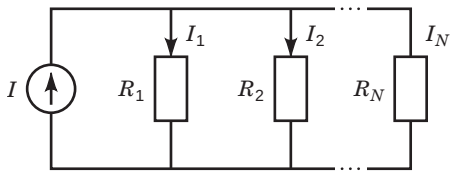

Figure 6. Parallel current divider.

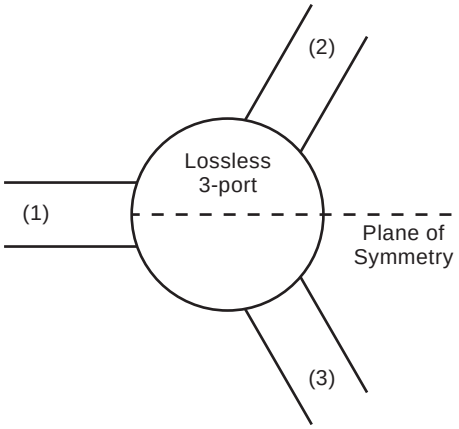

Figure 7. Lossless 3-port network.

where $[I]$ is the identity matrix, and the superscripts * and T represent complex conjugation and transpose, respectively. The symmetrical condition is defined by the following equations:

$$|S_{11}| = |S_{22}| = |S_{33}| = T \tag{17}$$

$$|S_{21}| = |S_{31}| = |S_{32}| = K \tag{18}$$

where T and K are constants. Substituting Eqs. (21) and (22) into Eq. (20), and after considerable algebraic manipulation, we obtain the following parameter values for the symmetrical case:

$$|S_{11}| = |S_{22}| = |S_{33}| = 1/3 \text{ or } -9.54 \text{ dB} \tag{19}$$

$$|S_{21}| = |S_{31}| = |S_{32}| = 2/3 \text{ or } -3.52 \text{ dB} \tag{20}$$

The latter analysis assumes that the S-parameter values are independent of frequency, but in actual practical design the S-parameter values vary significantly with frequency.

The 4-Port Transformer Circuit. In the schematic of a 4-port hybrid coil transformer circuit shown in Fig. 8, the primary transformer coil is linked to a center-tapped secondary coil (2). Assuming ideal transformers, the scattering matrix of the 4-port is determined as

$$[S] = \begin{bmatrix} \alpha & 0 & \beta & \beta \\ 0 & \alpha & \beta & -\beta \\ \beta & \beta & -\alpha & 0 \\ \beta & -\beta & 0 & -\alpha \end{bmatrix} \tag{21}$$

with

$$\alpha = \frac{1-2b}{1+2b} \tag{22}$$

and

$$\beta = \frac{2\sqrt{b}}{1+2b} \tag{23}$$

The constant b, as seen from Fig. 8, governs the relative turns ratio of the primary and secondary coils at ports 1 and 2, respectively. When the four ports are matched, i.e., $S_{ii} = 0$, $i = 1,4$ and the value of the constant $b = 0.5$, the scattering matrix from Eq. (25) reduces to the following simplified result:

$$[S] = \frac{1}{\sqrt{2}} \begin{bmatrix} 0 & 0 & 1 & 1 \\ 0 & 0 & 1 & -1 \\ 1 & 1 & 0 & 0 \\ 1 & -1 & 0 & 0 \end{bmatrix} \tag{24}$$

The performance of the hybrid coil circuit can be summarized qualitatively as follows:

- When a signal is input into port 1(3), it divides equally between ports 3(1) and 4(2) with a phase difference of 0°.
- When a signal is input into port 2(4), it divides equally between ports 3(1) and 4(2) with a phase difference of 180°.
- Ports 1 and 2 are isolated from one another.
- Ports 3 and 4 are isolated from one another.

Medium Frequency Power Dividers (Up to 1 GHz)

Two-Wire Transmission Line Power Dividers. A lossless power divider circuit is shown in Fig. 9, where Y_1, Y_2 and Y_3 denote the characteristic admittances of the respective transmission line sections. The input is matched by the condition $Y_1 = Y_2 + Y_3$, and the scattering matrix takes the form

$$[S] = \begin{bmatrix} 0 & \sqrt{\dfrac{Y_2}{Y_1}} & \sqrt{\dfrac{Y_3}{Y_1}} \\ \sqrt{\dfrac{Y_2}{Y_1}} & -\dfrac{Y_3}{Y_1} & \dfrac{\sqrt{Y_2 Y_3}}{Y_1} \\ \sqrt{\dfrac{Y_3}{Y_1}} & \dfrac{\sqrt{Y_2 Y_3}}{Y_1} & -\dfrac{Y_2}{Y_1} \end{bmatrix} \tag{25}$$

The power division is directly related to the admittance ratio

$$\frac{P_2}{P_3} = \frac{|S_{21}|^2}{|S_{31}|^2} = \frac{Y_2}{Y_3} \tag{26}$$

The device can provide either equal or unequal power split between the two output ports.

Coaxial Power Dividers. A general form of the coaxial tee junction is shown in Fig. 10 (1), in which port 3 is taken as the input port, and ports 1 and 2 are the output ports. The input impedance at port 3 is given by

$$Z_{i3} = Z_{03}^2 \left(\frac{Z_{L1}}{Z_{01}^2} + \frac{Z_{L2}}{Z_{02}^2} \right) \tag{27}$$

This component can be used in either of the following modes.

Equal Power Divider Mode. When the load impedances $Z_{L1} = Z_{L2} = Z_0$ and the characteristic impedances $Z_{01} = Z_{02}$, the power splits equally between output ports 1 and 2.

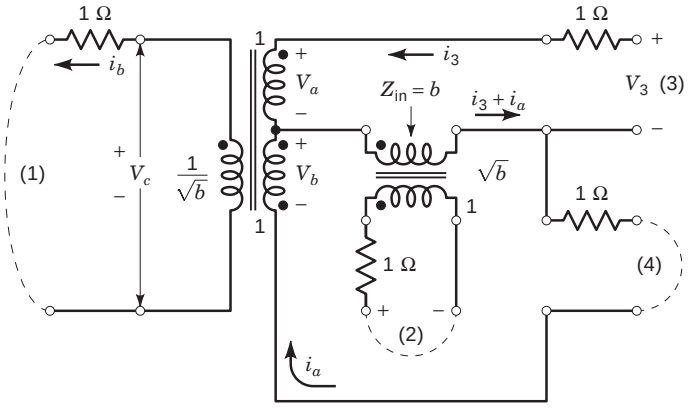

Figure 8. Hybrid coil circuit. (Reproduced with permission from H. J. Carlin and A. B. Giordano, *Network Theory, An Introduction to Reciprocal and Nonreciprocal Circuits,* Englewood Cliffs, NJ: Prentice Hall Inc., ©1964.)

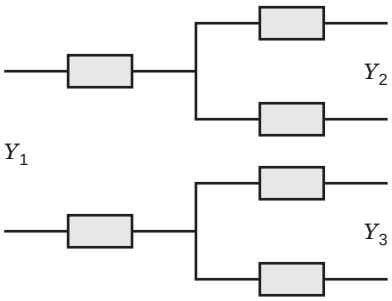

Figure 9. Lossless transmission line power divider: Y_1, Y_2 and Y_3 are the characteristic admittances of the input port 1 and output ports 2 and 3 respectively.

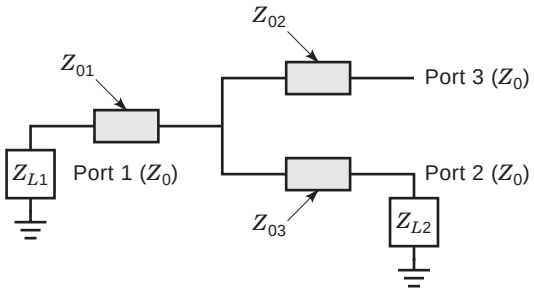

Figure 10. Coaxial tee junction: Z_{03}, Z_{02}, and Z_{01} are the characteristic admittances of the input port 3 and output ports 2 and 1, respectively.

Unequal Power Divider Mode. When the load impedances are match-terminated ($Z_{L1} = Z_{L2} = Z_0$), and the characteristic impedances at the two output ports are different, i.e., $Z_{01} \neq Z_{02}$, then unequal power division occurs between ports 1 and 2.

High-Frequency Power Dividers (1 GHz to 200 GHz)

Waveguide Power Dividers. Waveguide power divider circuits include 3-port and 4-port junctions as described in what follows.

Bifurcated Waveguide. This configuration, as shown in Fig. 11, is a rectangular guide containing a thin metal plate that divides the cross section of the guide into two guides having equal or unequal widths (1). The power division between output ports, when they are match-terminated, is

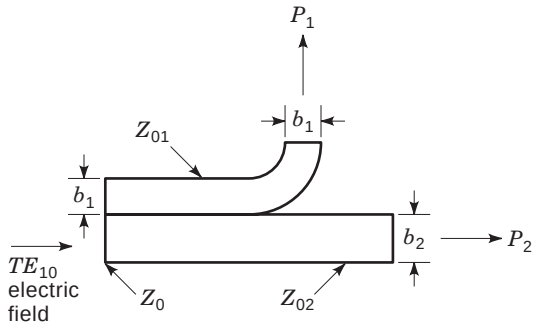

Figure 11. Bifurcated waveguide junction. Z_0 is the characteristic impedance of the input port and Z_{01} and Z_{02} are the characteristic impedances of the two output ports.

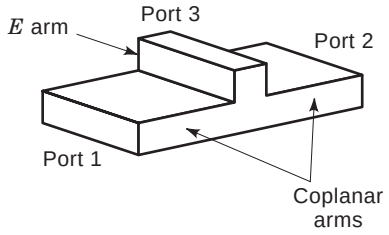

Figure 12. E-plane waveguide tee junction: Power from the input (port 3) divides equally in magnitude, but 180 degrees out of phase between the two outputs (ports 1 and 2).

given by the simple relation

$$\frac{P_1}{P_2} = \frac{Z_{01}}{Z_{02}} = \frac{b_1}{b_2} \tag{28}$$

Hence the bifurcated waveguide can be used as either an equal or unequal power divider.

E-Plane and H-Plane Waveguide Tee Junctions. These waveguide configurations, shown in Figs. 12 and 13, respectively, are both equal power dividers (1). The E-plane or series tee has equal power delivered to ports 1 and 2, which are called the coplanar arms, for a given power input into port 3, which is called the E arm. The electric field is delivered to output ports 1 and 2 equally in magnitude, and 180° out of phase if the lengths of the arms 1 and 2 are the same.

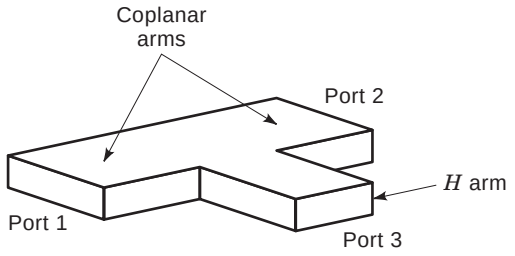

Figure 13. H-plane waveguide tee junction: Power from the input (port 3) divides equally in magnitude and phase between the two outputs (ports 1 and 2).

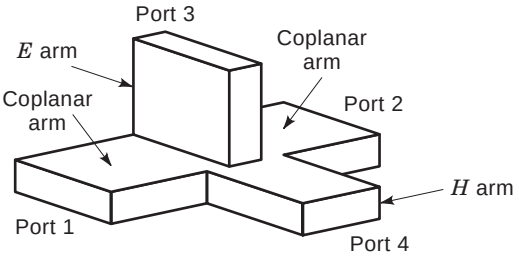

Figure 14. Hybrid (magic) tee junction: Power from input port 3 divides equally in magnitude, but 180 degrees out of phase between output ports 1 and 2, with zero output at port 4. Similarly, power from input port 4 divides equally in magnitude and phase between output ports 1 and 2, with zero output at port 3.

The H-plane tee is also known as a shunt tee, with port 3 designated as the H arm and ports 1 and 2 as the coplanar arms. A power input into port 3 splits equally between ports 1 and 2; if the lengths of the arms 1 and 2 are identical, the output electric fields are in phase.

Hybrid Magic Tee. This configuration is a 4-port network in which a signal incident on any one of the two input ports divides between two output ports with the other input port being isolated. The magic tee circuit can be considered a combination (hybrid) of the E-plane and H-plane tee as shown in Fig. 14. The important features of the magic tee operation are summarized here:

- All four ports are perfectly matched with voltage standing wave ratios (*VSWR*s) at a value of 1. Ports 3 and 4 and ports 1 and 2 are isolated from each other.
- A signal into the H arm divides equally between the coplanar arms, with zero° phase difference equidistant from the junction.
- A signal into the E arm divides equally between the coplanar arms, with 180° phase difference equidistant from the junction.

The scattering matrix for an ideal hybrid tee is as follows:

$$[S] = \begin{bmatrix} 0 & 0 & 1/\sqrt{2} & 1/\sqrt{2} \\ 0 & 0 & -1/\sqrt{2} & 1/\sqrt{2} \\ 1/\sqrt{2} & -1/\sqrt{2} & 0 & 0 \\ 1/\sqrt{2} & 1/\sqrt{2} & 0 & 0 \end{bmatrix} \tag{29}$$

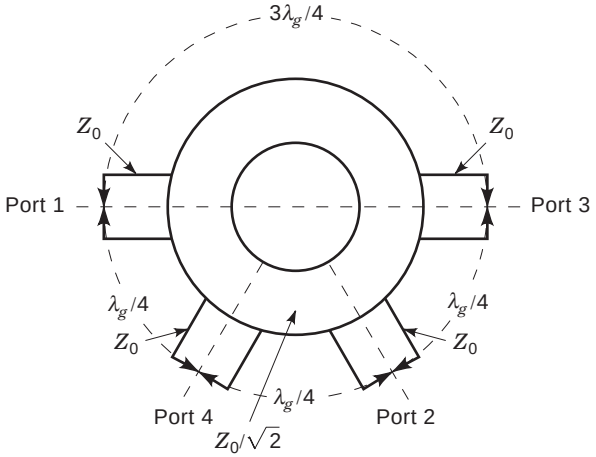

Figure 15. Waveguide hybrid ring: Power input at port 1 or port 2 splits equally between ports 3 and 4. Similarly, power input at port 3 or port 4 splits equally between ports 1 and 2.

Hybrid Ring. This hybrid junction also termed a rat race, has been developed in various configurations (3), including transmission line circuits. It consists of a waveguide ring, as shown in Fig. 15, having a mean circumference of $3\lambda_g/4$, and a characteristic impedance of $Z_0/\sqrt{2}$, where Z_0 is the characteristic impedance of the connecting guide. The following points summarize the operation of the hybrid ring:

- Ports 1 and 2 are decoupled.
- Ports 3 and 4 are decoupled.
- A signal entering port 1 or 2 splits equally between ports 3 and 4.
- By symmetry, a signal entering port 3 or 4 splits equally between ports 1 and 2.

Stripline Power Dividers. A classic N-port power divider is the *Wilkinson circuit* (4); the stripline version is shown in Fig. 16. The basic principle of operation, which also applies to the coaxial version, is the isolation of the two output ports through internally connected resistors. The input-output characteristics are summarized here:

- When a signal enters port 1, it divides equally in amplitude and phase between the output ports 2 and 3.
- When a signal input is applied to port 2 or 3, it divides equally between port 1 and resistor R, with zero signal appearing at the other port (3 or 2).
- When the characteristic impedance of the quarter-wave lines is $\sqrt{2}Z_0$, the input is matched when ports 2 and 3 are match-terminated.

Microstrip Power Dividers. Because the microstrip tee junction is a fundamental passive component in microwave and millimeter-wave monolithic circuits, the characterization of its transmission and reflection properties is a topic of considerable importance. The symmetrical 50 Ω tee junction is shown in Fig. 17, where all the arms of the 3-port

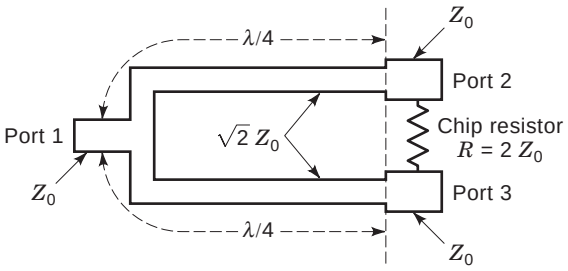

Figure 16. Wilkinson two-way power divider with equal power division: Power input at port 1 divides equally between output ports 2 and 3, which are isolated from each other by the resistor R.

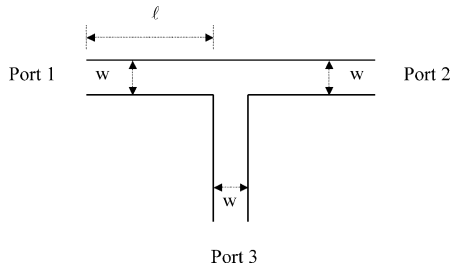

Figure 17. Basic 50 Ω tee junction.

network have an impedance of 50 Ω. The 50 Ω tee, which is also called an uncompensated design, is used as a basis for comparison with newer designs of compensated equal and unequal microstrip tee junction power dividers.

In comparison to the symmetrical 3-port junction, the compensated and uncompensated microstrip designs have ports 1 and 2 that are symmetrical to port 3. The passivity condition $[S]^{\mathrm{T}}[S]^{*} = [I]$ still holds but Eqs. (3) and (4) reduce to the following result:

$$|S_{11}| = |S_{22}| \tag{30}$$

$$|S_{31}| = |S_{32}| \tag{31}$$

in addition to the reciprocal condition

$$|S_{ij}| = |S_{ji}|, i, j = 1, 3 : i \neq j \tag{32}$$

Equations (<xref target="W6128-mdis-0034 W6128-mdis-0035 W6128-mdis-0036" style="unformatted"/>), substituted in Eq. (20) yield the following important power divider relations:

$$2|S_{31}|^2 + |S_{33}|^2 = 1 \tag{33}$$

and

$$|S_{21}|^2 - |S_{31}|^2 = |S_{33}|^2 - |S_{11}|^2 \tag{34}$$

The simulated scattering parameters of a basic uncompensated 50 ohm tee are graphically represented in Fig. 18. The dielectric substrate material is Teflon with a dielectric constant of $\varepsilon_{\mathrm{r}} = 2.17$, substrate thickness $h = 0.0508$ cm, and the width of the 50 Ω microstrip line is $w = 0.1534$ cm. The simulation was performed on Touchstone software (5), which utilizes the 3-port model of Hammerstad (6). Hammerstad's model is applicable for the general nonsymmetrical tee junction circuit shown in Fig. 19(a), in which the three arms of the junction can have different characteristic impedances. The equivalent circuit parameters, for the model in Fig. 19(b), are obtained from the junction dimensions through the key equations given as follows:

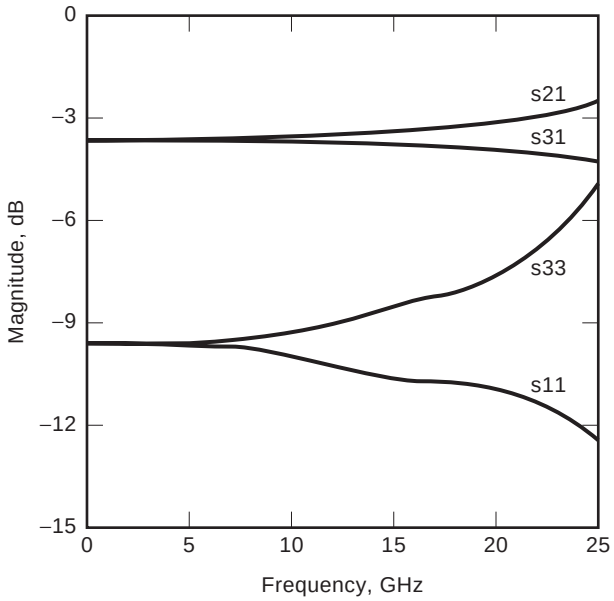

Figure 18. Scattering parameters of basic 50 Ω tee junction ($e_{\mathrm{r}} = 2.17$, $h = 0.0508$ cm, $w = 0.1534$ cm).

Turns ratio

$$n_{a,b}^2 = 1 - \pi \left(\frac{f}{f_{p1}}\right)^2 \left[\frac{1}{12}\left(\frac{Z_{1a,b}}{Z_2}\right)^2 + \left(0.5 - \frac{d_2}{D_1}\right)^2\right] \tag{35}$$

Shunt susceptance

$$\frac{B_T}{Y_2}\frac{\lambda_1}{D_1} = 5.5\frac{\epsilon_r + 2}{\epsilon_r}\left[1 + 0.9\ln\frac{Z_1}{Z_2} + 4.5\frac{Z_1}{Z_2}\left(\frac{f}{f_{p1}}\right)^2 - 4.4\exp\left(-1.3\frac{Z_1}{Z_2}\right) - 20\left(\frac{Z_2}{\eta_0}\right)^2\right] n^{-2}\frac{d_1}{D_2} \tag{36}$$

Other earlier approaches to T junction modeling include the development of equivalent circuit models by Oliner (7), Silvester and Benedek (8), Wheeler (9); the frequency response of the equivalent circuits was obtained. However, because these methods are based on static approximations, they are considered valid with sufficient accuracy only at low frequencies. Menzel and Wolf (10) developed a waveguide model for symmetrical and nonsymmetrical T junctions, in which the electric and magnetic fields of the microstrip T are expanded in terms of TEM and $\mathrm{TE}_{\mathrm{no}}$ modes. The boundary conditions are then solved to obtain the frequency dependence of the S parameters. The numerical calculations on asymmetrical T junctions showed good agreement with experimental results up to ~ 12 GHz. This model ultimately led to the full-wave spectral domain analysis for the T junction by Wu et al. (11), which takes into account all physical effects, including radiation and surface waves.

The full-wave analysis for microstrip junction problems defines the module as the region where higher-order modes

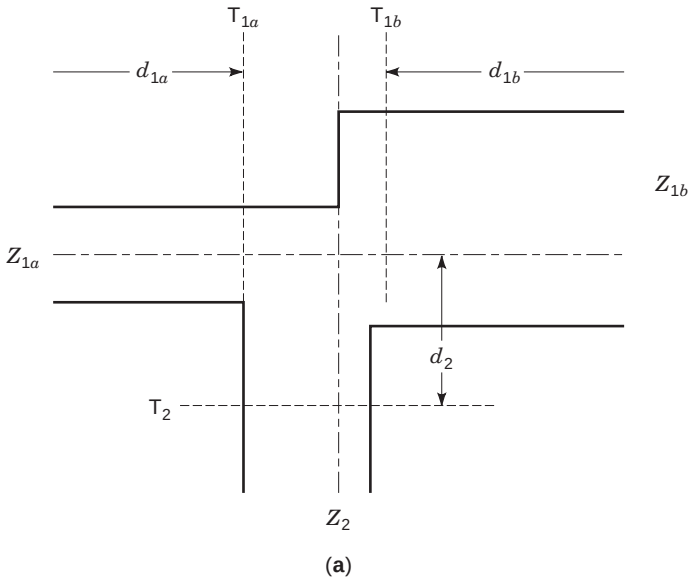

(a)

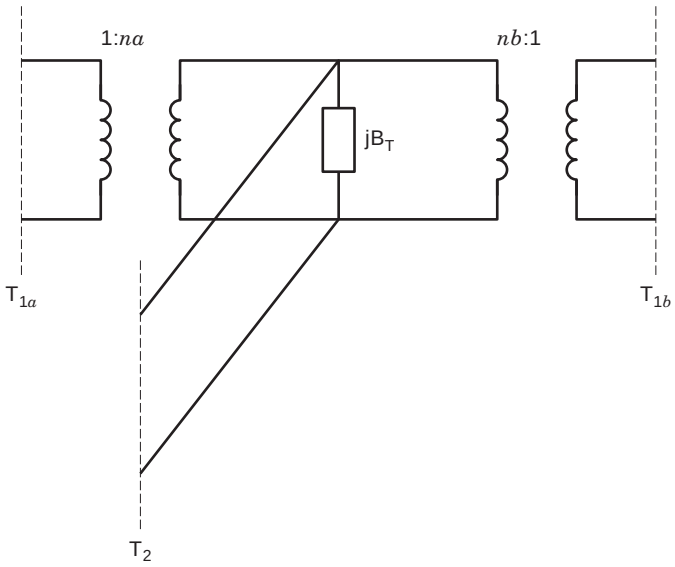

(b)

Figure 19. (a) Generalized nonsymmetrical tee junction. (Reproduced with permission from E. Hammerstad, Computer-aided design of microstrip couplers with accurate discontinuity models, *IEEE Microw. Theory Tech. Symposium Digest,* 54–56, © 1981 IEEE.) (b). Equivalent circuit of nonsymmetrical tee junction. (Reproduced with permission from E. Hammerstad, Computer-aided design of microstrip couplers with accurate discontinuity models, *IEEE Microw. Theory Tech. Symposium Digest,* 54–56, © 1981 IEEE.)

are generated. The currents inside the module are expanded in terms of piecewise- sinusoidal-pulse (*PWS-P*) or piecewise triangular basis functions, while the currents outside the module are uniform transmission line currents [semiinfinite mode (*SIM*)]. Consequently, the electric fields are constructed from the unknown currents on the microstrip as

$$E_x(x,y) = \iint G_{xx}J_x(x_s,y_s)\,dy_s\,dx_s + \iint G_{xy}J_y(x_s,y_s)\,dy_s\,dx_s = 0 \tag{37}$$

$$E_y(x,y) = \iint G_{yx}J_x(x_s,y_s)\,dy_s\,dx_s + \iint G_{yy}J_y(x_s,y_s)\,dy_s\,dx_s = 0 \tag{38}$$

where G_{xx}, G_{xy}, G_{yx} and G_{yy} are the spatial-domain dyadic Green's functions. A nearly Galerkin method is applied to transform the integral equations into matrix equations. The matrix equation is of the form

$$[Z][I] = [V_{in}] \tag{39}$$

where the elements of $[Z]$ represent the reaction between the basis function of the current expansion. $[V_{\text{in}}]$ is in the same mathematical form as $[Z]$, except that the basis function is the semiinfinite mode of the incident wave.

Equal Power Divider Designs. A fundamental occurrence in the S parameter characteristics of the uncompensated 50 Ω tee junction, as seen from Fig. 18, is that the predicted insertion loss of −3.52 dB beween ports 1-2 and 1-3 is not maintained over the frequency band 1–10 GHz. As the fre-

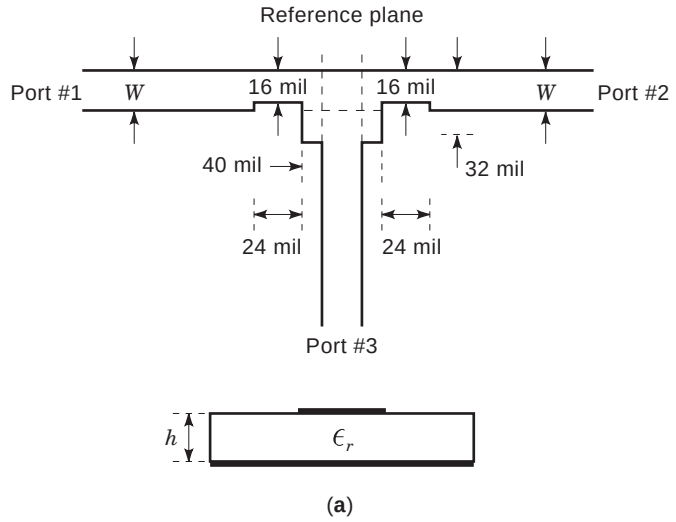

(a)

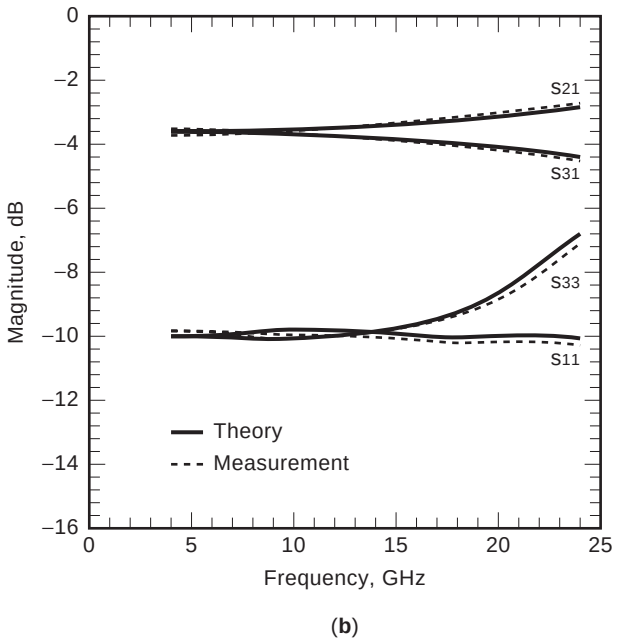

(b)

Figure 20. (a) Schematic of shaped T junction, $\varepsilon_r = 9.9$, $h = 0.0638$ cm. (b) Scattering parameters of shaped T junction. (Reproduced with permission from S. Wu, H. Yang, N. G. Alexopoulos, I. Wolff, A rigorous dispersive characterization of microstrip cross and T junctions, *IEEE Trans. Microw. Theory Tech., 38*(12):1837–1844, © 1990 IEEE.)

quency is increased, it is noted that more power flows to port 2 than to port 3 and the VSWR is degraded at each port. Hence, modifications in the structure of the basic 50 Ω tee are made to compensate for the power flow mismatch at the two output ports. One approach is to shape the basic 50 Ω tee (11) as shown in Fig. 20(a). The simulated (through full-wave analysis) and measured characteristics of the compensated tee, as depicted in Fig. 20(b), clearly demonstrate the improvement in power match at ports 2 and 3.

Unequal Power Divider Design. The aim of unequal power design (12) is to compensate or modify the basic 50 Ω T, shown in Fig. 17, to maintain a prespecified difference, i.e.,

$$|S_{21}| - |S_{31}| = k\,dB \tag{40}$$

over a desired frequency band. The various empirical models that have evolved through analysis and computer aided simulation, include the following microstrip circuits.

Asymmetrical Tee. The asymmetrical tee, as shown in Fig. 21, is the simplest approach to the unequal power divider (13). The width of orthogonal arm 3 is fixed at the nominal 50 Ω width, but the widths of the collinear arms are varied according to the value of k dB in Eq. (44). The dimensions of the circuit are optimized by the Gradient Least Squares Optimizer on the EEsof Touchstone simulation software (5). This software was the predecessor to the currently available Agilent Advanced Design System (ADS). The width and the length of the orthogonal arm were fixed at $w = 0.1534$ cm (corresponding to a characteristic impedance of $Z_0 = 50$ Ω) and $\ell = 2$ cm, respectively. These dimensions correspond to a material dielectric con-

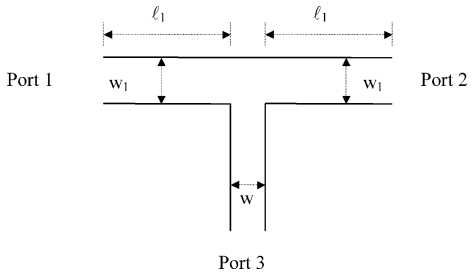

Figure 21. Asymmetrical T junction.

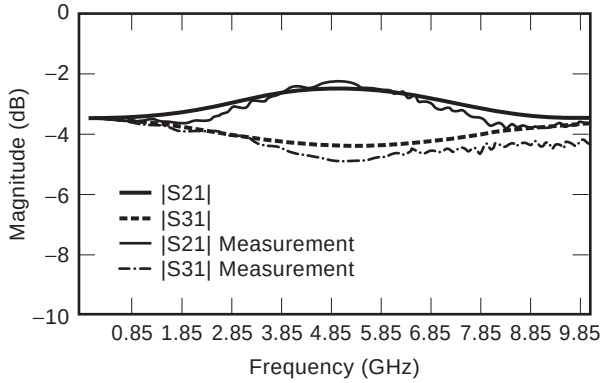

Figure 22. Scattering parameters of asymmetrical T junction for k = 1.5 dB (e_r = 2.17, h = 0.0508 cm, w = 0.1534 cm).

stant of ε_r = 2.17, and a substrate thickness of h = 0.0508 cm. The least-squares optimization problem, as executed by the Touchstone Optimizer, can be summarized as follows for a value of k = 1.5 dB.

The objective function is

$$\begin{aligned} |S_{31}| &= -4.27 \text{ dB } (-3.52 - 0.75) \\ |S_{21}| &= -2.77 \text{ dB } (-3.52 + 0.75) \end{aligned} \tag{41}$$

at N frequencies f_i, i = 1, 2 ... N in the frequency range of 1–8 GHz. Then the error E to be minimized is defined as

$$E = E_1 + E_2 \text{ (dB)}$$

where

$$E_1 = \sum_{i=1}^{N} [|S_{31}|_{f=f_i} - (-4.27)]^2/N \tag{42}$$

and

$$E_2 = \sum_{i=1}^{N} [|S_{21}|_{f=f_i} - (-2.77)]^2/N$$

The optimized dimensions of the asymmetrical T junction are displayed in Table 1 for two cases of power division, k = 1.5 dB and k = 3 dB. Based on these design parameters, the microstrip circuits were fabricated (13), and tested for the scattering parameters on the HP 8510B Automatic Network Analyzer. The simulated and measured transmission scattering parameters are compared in Figs. 22 and 23 for the two cases of k = 1.5 dB and k = 3 dB, respectively.

From the scattering parameter curves, it is seen that the asymmetrical tee unequal power-divider acts essentially as a *narrowband circuit,* with the separation k dB maintained

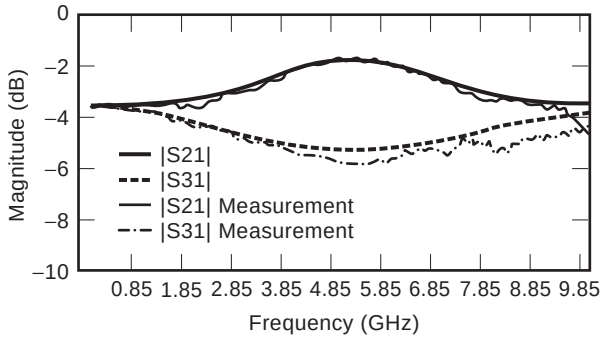

Figure 23. Scattering parameters of asymmetrical T junction for k = 3.0 dB (e_r = 2.17, h = 0.0508 cm, w = 0.1534 cm).

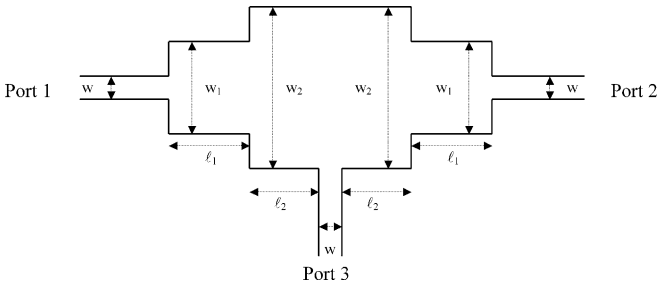

Figure 24. 2-step T junction.

only over a small portion of the band. One useful figure-of-merit to specify the bandwidth of operation of the junction is defined as the 0.5 dB bandwidth, which is the point at which the value of k drops from a peak value to a value of 0.5 dB below peak.

Stepped Tee Junction. In order to improve the performance bandwidth of the asymmetrical tee, the 2-step model evolved (13) as shown in Fig. 24. The stepped microstrip T junction was considered earlier by Menzel and Wolf (10), who used the compensation to make the reflection coefficient at port 3 zero at a particular frequency. The optimization approach, as described in the previous section for the asymmetrical tee, was adopted to optimize the step widths, $w1$, $w2$, and the step lengths $\ell 1$ and $\ell 2$, in order to achieve the objective function k dB over the frequency band of 1–8 GHz. The results of the Touchstone Gradient Optimizer are summarized in Table 2 for two specific values of k = 1.5 dB and k = 3 dB.

The rms error E for the 2-stepped T is much reduced as compared with the error for the asymmetrical T, which depicts that the 2-stepped T has a much closer match to the objective function of the optimization problem. The simulated and measured scattering transmission parameters are compared in Figs. 25 and 26 for the cases of k = 1.5 dB and k = 3 dB, respectively.

Tapered T Junction. Another broadband unequal power divider circuit is the linearly tapered microstrip T junction circuit (13) shown in Fig. 27. In this case the objective function also remains the same, i.e., $|S_{21}| - |S_{31}| = k$ dB (prespecified), over the frequency band of 1–8 GHz. The optimized dimensions of the tapered width w1 are listed in

Table 2. Optimized Dimensions of 2-Step Tee Junction

$\lvert S_{21}\rvert - \lvert S_{31}\rvert$, dB	$w1$(cm)	$w2$(cm)	$\ell 1$(cm)	$\ell 1$(cm)	rms Error E (dB)
1.5	0.1831	0.2255	1.0723	1.0147	0.0533
3.0	0.2148	0.3116	1.0413	1.0553	0.3114

Table 1. Optimized Dimensions of Asymmetrical Tee Junction

$\lvert S_{21}\rvert - \lvert S_{31}\rvert$, dB	$w1$ (cm)	$\ell 1$(cm)	rms Error E (dB)
1.5 dB	0.2102	0.9981	0.1794
3.0 dB	0.2705	0.9426	1.2453

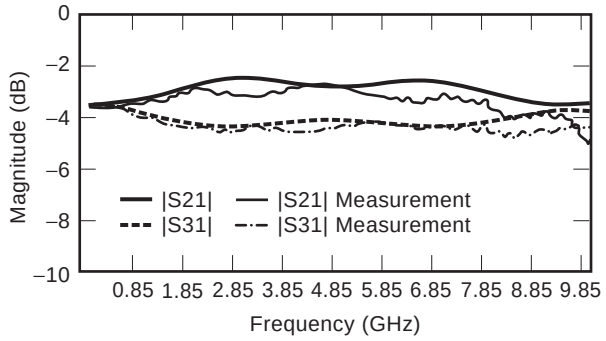

Figure 25. Scattering parameters of 2-step T junction for k = 1.5 dB (e_r = 2.17, h = 0.0508 cm, w = 0.1534 cm).

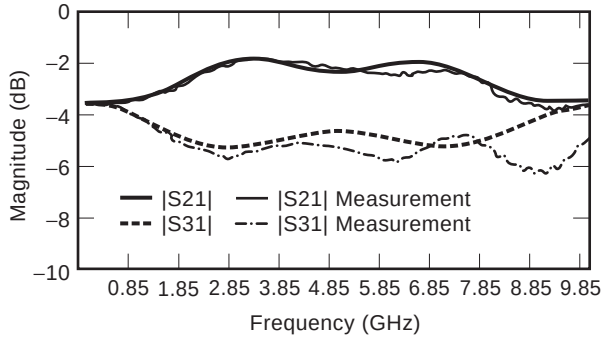

Figure 26. Scattering parameters of 2-step T junction for k = 3.0 dB (e_r = 2.17, h = 0.0508 cm, w = 0.1534 cm).

Table 3 for two cases of power division, k = 1.5 dB and 3 dB.

The simulated and measured scattering parameters are compared in Figs. 28 and 29 for the two cases of power division k = 1.5 dB and k = 3 dB, respectively. On comparison of Tables 2 and 3, it is seen that the rms error is ∼ half of the rms error for the 2-stepped T circuits. The tapered tee circuit characteristics are flat over frequencies greater than ∼ 1.50 GHz, whereas the 2-step T tee has a more gradual cut-off at frequencies < 2.5 GHz. However, the transmission characteristics for the tapered T deteriorate towards the end of the band (1–8 GHz).

Empirical Models for Microstrip Unequal Power Dividers. The development of the three unequal power divider circuits, the asymmetrical tee, the stepped tee, and the linearly tapered tee, led to the generation of considerable simulated and measured data on their transmission characteristics. These data were used as a basis to develop the following empirical design Eqs. (18) for the circuit dimensions, given a certain desired power divider ratio $k = \lvert S_{21}\rvert - \lvert S_{31}\rvert$, dB over a frequency band of interest.

Asymmetrical T. The circuit dimensions held constant, from Fig. 21, are ℓ = 2 cm, $\ell 1$ = 1 cm, and w = 0.1534 cm. The design equation for the width $w1$ is given by:

$$w1 = 0.036\,k + 0.1534 \tag{43}$$

where k, the specified power divider ratio is in decibels, and $w1$ is in centimeters.

Stepped Tee. The circuit dimensions held constant, from Fig. 24, are ℓ = 2 cm, $\ell 1 = \ell 2$ = 1 cm and w = 0.1534 cm. The design equation for the width $w1$ is given by

$$w1 = 0.0187\,k + 0.1534 \tag{44}$$

and for the width $w2$

$$w2 = 0.0468\,k + 0.1534 \tag{45}$$

where $w1$, $w2$ are in centimeters and k is in decibels.

Linearly Tapered Tee. The circuit dimensions held constant, from Fig. 27, are ℓ = 2 cm, $\ell 1$ = 3 cm and w = 0.1534 cm. The design equation for the width $w1$ is given by

$$w1 = 0.0694\,k + 0.1534 \tag{46}$$

where $w1$ is in centimeters and k is in decibels.

Optical Power Dividers (THz)

Symmetric Optical Dividers. Symmetric optical couplers can be used either as power splitters or power combiners (15). A splitter configuration is shown in Fig. 30(a). Under ideal conditions, input power at port 1 or 2 splits equally between ports 3 and 4, i.e., $P_3 = P_4 = P_1/2$ or $P_2/2$. A combiner configuration is shown in Fig. 30(b), ideally in which,

Table 3. Optimized Dimensions of Linearly Tapered Tee Junction

$\lvert S_{21}\rvert - \lvert S_{31}\rvert$, dB	$w1$ (cm)	ℓ (cm)	rms Error (dB)
1.5	0.2456	3.00	0.0263
3.0	0.3658	3.00	0.1549

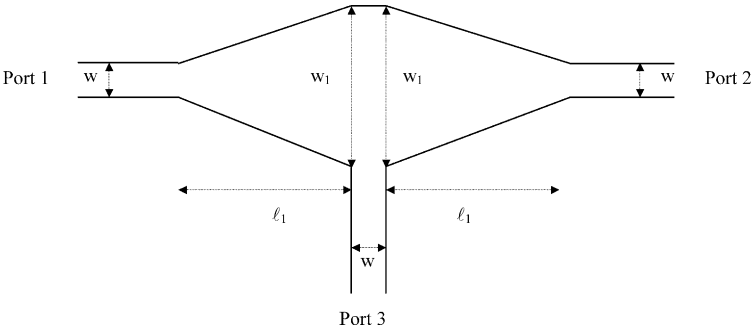

Figure 27. Linearly tapered microstrip T junction.

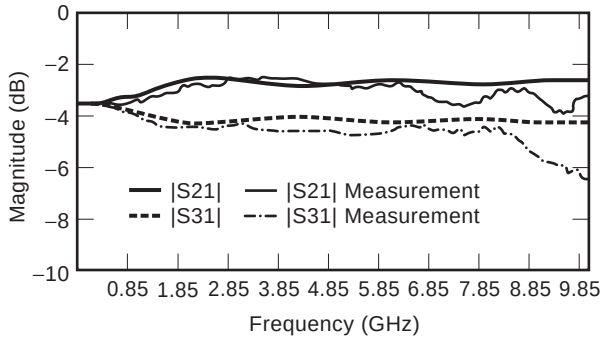

Figure 28. Scattering parameters of tapered T junction for k = 1.5 dB (e_r = 2.17, h = 0.0508 cm, w = 0.1534 cm).

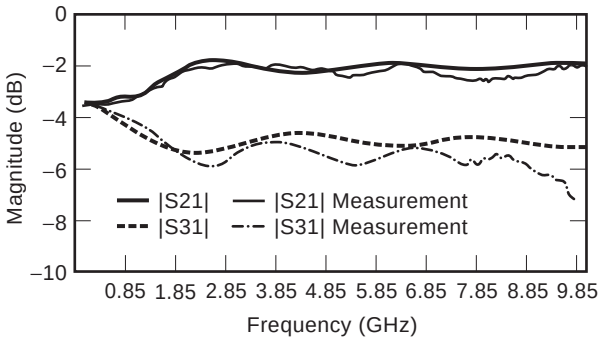

Figure 29. Scattering parameters of tapered T junction for k = 3.0 dB (e_r = 2.17, h = 0.0508 cm, w = 0.1534 cm).

however, $P_1 = P_2 = P_3/2 + P_4/2$ due to the power being divided symmetrically between ports 1 and 2.

Asymmetric Optical Dividers. Asymmetrical splitters and combiners are constructed from multimode fibers having different core sizes as shown in Fig. 31, with the cladding thickness assumed negligible. In either configuration, the governing power law is $P_1 = P_2 + P_3$.

FUTURE TRENDS IN POWER DIVIDERS

Power dividers are one of the most important elements for the transmission and distribution of power ranging in frequency from dc to optical (THz). As electrical devices become increasingly smaller, research on miniaturized components with comparable performance to traditional circuits is essential. Another important direction in power divider research is the development of advanced computer simulation tools with the capacity of accurate device characterization, which is fundamental to the realization of efficient designs.

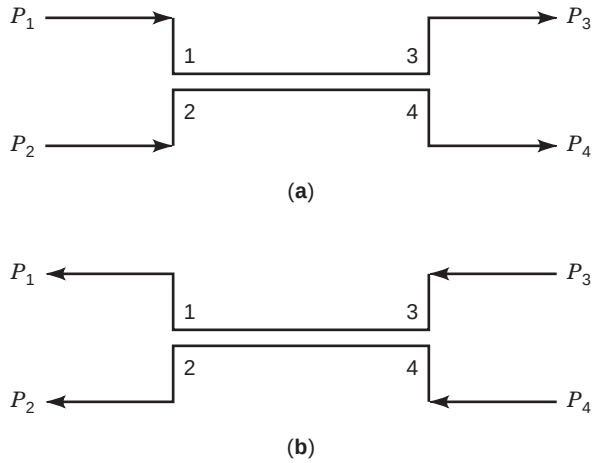

Figure 30. (a) Symmetric optical power splitter: Input ports 1, 2 and output ports 3, 4. (b) Symmetric optical power combiner: Input ports 3, 4 and output ports 1, 2.

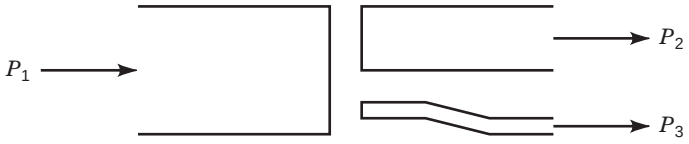

Figure 31. Asymmetric optical power splitter/combiner: The power equation in both splitter and combiner mode is $P_1 = P_2 + P_3$.

BIBLIOGRAPHY

P. A. Rizzi *Microwave Engineering-Passive Circuits*, Englewood Cliffs, New Jersey: Prentice Hall Inc., 1988.

2. H. J. Carlin A. B. Giordano *Network Theory: An Introduction to Reciprocal and Non-Reciprocal Circuits*, Englewood Cliffs, New Jersey: Prentice Hall Inc., 1964.
3. W. A. Tyrell Hybrid circuits for microwaves, Proc. IRE,35 (11):1294–1306, 1947.
4. E. J. Wilkinson An N-way hybrid power divider, IRE Trans. Microw. Theory Tech.,8 (1):116–118, 1960.
5. Touchstone/DOS Reference, Ver. 3.0, LEL-101, 1991.
6. Computer-aided design of microstrip couplers with accurate discontinuity models, IEEE Microw. Theory Tech. Symposium Digest, 54–56, 1981.
7. A. A. Oliner Equivalent circuits for discontinuities in balanced strip transmission line, IEEE Trans. Microw. Theory Tech.,3(11):134–143, 1955.
8. P. Silvester P. Benedek Microstrip discontinuity capacitances for right-angle bends, T junctions and crossings, IEEE Trans. Microw. Theory Tech.,21 (5):341–346, 1973.
9. H. A. Wheeler Transmission-line properties of parallel strips separated by a dielectric sheet, IEEE Trans. Microw. Theory Tech.,13 (3):172–185, 1965.
10. W. Menzel I. Wolff A method of computing the frequency-dependent properties of microstrip discontinuities, IEEE Trans. Microw. Theory Tech.,3 (2):107–112, 1977.
11. S. Wu *et al.* A rigorous dispersive characterization of microstrip cross and T junctions, IEEE Trans. Microw. Theory Tech.,38 (12):1837–1844, 1990.
12. M. Villegas *et al.* Analysis and design of microwave T junction circuits for prescribed response characteristics, Proc. 36th Midwest Symp. on Circuits and Systems, 604–605, 1993.
13. B. P. Kumar *et al.* Optimization of microwave T junction power divider circuits, Proc. 37th Midwest Symp. on Circuits and Systems, 1994.
14. G. R. Branner B. P. Kumar D. James Design formulae for a class of microstrip tee junction power divider circuits, Proc. of the 39th Midwest Symp. on Circuits and Systems, 1996.
15. F. C. Allard (ed.) *Fiber Optics Handbook for Engineers and Scientists*, New York: McGraw-Hill, 1990.

B. P. KUMAR
G. R. BRANNER
G. RAZMAFROUZ
D. BRODY
University of California, Davis,
Davis, CA, 95616 3123
Engineering II